TEMPORAL INSTABILITY OF NON-NEWTONIAN LIQUID JETS DURING CENTRIFUGAL ELECTROSPINNING

by

Abdullah Madhi ALSHARIF*

Department of Mathematics and Statistics, College of Science,
Taif University, Taif, Saudi Arabia

Original scientific paper
https://doi.org/10.2298/TSCI22S1157A

This investigation is aimed at analysing linear instability of an initial stable jet through the air-sealed electro-centrifugal spinning process which is significant in creating nanofibers. Utilising the perturbation theory to diminish the governing equations, into a 1-D mode with the option of solving acquired non-linear differential equations. Hence, the trajectory of a power-law fluid jet during electro-centrifugal spinning power has been determined. Dispersion relation has been gotten from the linear theory to study the conduct of a power-law fluid curved jet with an electric field.

Key words: *instability, centrifugal spinning, liquid jets, electric field*

Introduction

A charged spinning fluid jet is of enthusiasm for scholarly and engineering applications, for example, ink-jet printers, fuel spraying, microencapsulation, and electro-spinning.

The early works in this subject were led tentatively by Savart [1], yet he did not decipher the reason for the instability. Plateau [2] found that surface strain is the kay factor of the jet decay. Rayleigh hypothetically treatment the instability of incompressible inviscid fluid jets [3] and it was found that surface tension leads to instability. The linear instability examination of fluid jets was inspected by Middleman [4] to investigate the conduct of the instability in laminar and turbulent jets emerging from a nozzle.

From that point forward, the linear instability (LIS) of non-Newtonian fluid (NNF) jets have been carried out by a large number of authors. For example, a mathematical report has been utilized by Renardy [5] to observe drop formation of Newtonian state and viscoelastic fluid jets for both constitutives of the upper convected Maxwell and the Giesekus. Middleman [4] has looked at how stable viscoelastic jets are. Between inviscid, Newtonian, and viscoelastic fluid jets, Goldin *et al*. [6] contrasted the linear stability of each type. Brenn *et al*. [7] likewise explored the linear instability (LI) of axisymmetrical NNF jets. As indicated by their examination, LIS shows that viscoelastic jets exhibit more instability than Newtonian jets with a similar Ohnesorge number. When studying the rheological behavior of polyisobutylene and polystyrene at low shear rates, Larson [8] utilized the Oldroyd-B model for perfect elastic fluids (also known as Boger fluids). Schummer and Thelen [9] investigated the break-up of a viscoelastic fluid jet by utilizing Jeffrey's model and researched LS. According to Larson [10], both non-Newtonian and Newtonian fluids exhibit linear and non-linear instability. The mathemati-

* Author's e-mails: abu.madhi@hotmail.com, a.alshrif@tu.edu.sa

cal investigation was led by Li and Fontelos [11] for BOSS for viscoelastic fluid jets by utilizing an unequivocal finite difference technique and the others [12-14].

The elements of BOSS and lament thread have been talked about by Ardekani *et al*. [15] for weakly viscoelastic jets by utilizing the Giesekus main relation and their results contrast with the Oldroyd-B model (when $\alpha = 0$) and the other works [16-18]. Moreover, the instability of Newtonian and non-Newtonian jets during centrifugal spinning have been studied by numerous scientists, for example, Divvela *et al*. [19], Alsharif [20], Taghavi and Larson [21], Alsharif *et al*. [22], and Riahi [23]. Nanofiber arrangement during centrifugal jet spinning (CJS) within the sight of gravity was analyzed by Noroozi *et al*. [24], and they utilized in this examination the power-law model. Polymers nanofibers have numerous applications in different territories, so for additional details, the intrigued perusers can go to the investigation of Rogalski *et al*. [25].

The process of CJS has been analyzed broadly in literature with respect to the linear and non-linear instability of uncharged fluid jets, which is urgent for understanding the break-up of fluid jets. Various researchers utilized the linear theory to give a superior comprehension of the components of creating fiber jets by applied electric fields. Hohman *et al*. [26] considered the temporal instability of an electrically powered jet. They utilized a 1-D model of Newtonian charged fluid jet, and they likewise inferred the dispersion relation examine the effects of specific parameters on the conduct of the linear instability of direct jets. Hohman *et al*. [27] determined the steady-state arrangements of viscous fluid jets of their prior work [20]. Alsharif and Parau *et al*. [28] discussed the centrifugal spinning viscous jet in the presence of electric field. The span along the fluid jet has been represented within the sight of different estimations of dimensionless parameter Rb and E_∞. Moreover, a small travelling wave mode has been considered around the steady-state answers, that are raveled in their steady-state solutions, creating a small perturbation in these solutions as shown in Alsharif and Parau *et al*. [28], see eq. (6.1). Furthermore, the perturbation eq. (6.1) are used to substitute into the governing steady equations. We therefore, get the dispersion relation at leading order as seen in eq. (6.3).

The influence of the presence of an electric field on Newtonian and non-Newtonian fluid jets in the electro-spinning process has been inspected by Feng [29]. He additionally showed the connection between the electric field, surface charge, and the jet radius along with the jet.

There are numerous authors, who portrayed the components of the linear temporal stability theory of non-Newtonian fluid jets in the appearance or absence of the electric field. Among them, Reneker *el al*. [30] and Yarin *et al*. [31] built up a viscoelastic model to concentrate mathematically on the non-linear instability of a jet during electro-spinning. Carroll and Joo [32] analyzed the linear axisymmetric instability of an electric field viscoelastic jet.

A non-Newtonian polymeric fiber jet during the power spinning (FS) process was analyzed by Riahi [23]. He decreased the governing framework equations utilizing the asymptotic methodology for the jet flow and built up a polymeric fluid model, and afterward, the steady-state arrangements are found to determined the jet trajectory during this process.

New test results on the effect of joining power spinning with electro-spinning on viscoelastic jets were acquired as of late by Chang *et al*. [33] and Liao *et al*. [34]. There are just a couple of hypothetical outcomes on the bonded effect of power spinning along the electro-spinning, (see Riahi [35], for instance, who considered the reaction of an electric force on the steady non-Newtonian jets).

The point of this examination is to inspect the linear instability of axisymmetric power-law fluid jets within the sight of centrifugal spinning and electric fields. In the following segment, we will consider the power-law model to get the numerical detailing. At that point, an asymptotic methodology is considered to get the steady-state arrangements utilizing the

Rong-Kutta strategy. At last, the dispersion relation is determined to consider the conduct of the centrifugal spinning and electric field on the development rate and the wavenumber of fluid jets.

Model development

To evaluate the impact of centrifugal force on the viscous fluid jets during outward rotation, it is supposed that there is a cylindrical container rotation containing an angular velocity Ω of radius s_0. Around that axis, the container as well as the axis rotate. On its side is a slight opening (radius a) on the container.

The Cartesian framework co-ordinates x, y, z rotate along the container. In this edition, the x- and z-axes are each perpendicular and tangential to the outside of the cylinder. As we are keen on quickly rotating jets, the significance of the gravitational force is minute, so we disregard the power of gravity in this issue. We employ the capacity, $x = X(s, t)$, z = $Z(s, t)$ in order to describe the location of the centerline of the curved fluid jet that travels in the plane $y = 0$, see [36, 37]:

$$\begin{gathered} \nabla u = 0 \\ \rho\left(\frac{\partial u}{\partial t} + u\nabla u\right) = \nabla\tau - 2w\times u - w\times(w\times r) \\ \tau = \tau^F + \tau^E \\ \tau^F = \eta\gamma \end{gathered} \tag{1}$$

where u is the presented as the velocity of form $u = ue_s + ve_n + we_\phi$, regarding ρ as the fluid density, and r is the position vector of any particle, expressed as $r = \int_0^s e_s ds + ne_n$, and p is the pressure. The container's angular velocity is w, γ is the rate of strain tensor. The formula $\eta = m\,[(\gamma{:}\gamma)/2]^{(\alpha-1)/2}$ is the apparent viscosity, and α is the flow index number. We also define ϵ_2 as the dielectric constant/ permittivity of the air [38]. The liquid surface are [39]:

$$\nabla(\epsilon_1 E) = q \tag{2}$$

$$\frac{\partial Q}{\partial t} + u\nabla_s Q - Qn(n\nabla)u = [KEn]_2^1 \tag{3}$$

where ∇_s, n, and q are correspond to the surface gradient operator and Q is the motion of surface charge, the (outward) normal unit vector to the liquid jet and the free charge density in the fluid, respectively.

Steady-state solutions

The asymptotic slender jet is employed in order to obtain the steady-state answers, Eggers [40]:

$$u = u_0(s,t) + (\epsilon n)u_1(s,\phi,t) + \cdots$$

$$v = (\epsilon n)v_1(s,\phi,t) + (\epsilon n)^2 v_2(s,\phi,t)\cdots$$

$$p = p_0(s,t) + (\epsilon n)p_1(s,\phi,t) + \cdots$$

$$R = R_0(s,t) + (\epsilon)R_1(s,\phi,t) + \cdots$$

$$Q = Q_0(s,t) + (\epsilon)Q_1(s,\phi,t) + \cdots$$

$$X = X_0(s) + (\epsilon)X_1(s,t) + \cdots$$

$$Z = Z_0(s) + (\epsilon)Z_1(s,t) + \cdots$$

$$(E_s, E_n, E_\phi) = (E_0, 0, 0)(s,t) + (\epsilon n)(E_{s1}, E_{n1}, E_{\phi 1})(s,\phi,t) + \cdots$$

We can note that this specified method was applied in the subject of curved liquid jets as seen in Decent *et al*. [37, 41] and Uddin *et al*. [42]. Instead of writing X_0, Y_0, and Z_0, X, Y, and Z can be cited.

The governing equations which describe the flow can be written:

$$h_s\left(\epsilon\frac{\partial u}{\partial t}+\epsilon(v\cos\phi - w\sin\phi)g + v\frac{\partial u}{\partial n}+\frac{w}{n}\frac{\partial u}{\partial \phi}\right)+\epsilon u\frac{\partial u}{\partial s}+\epsilon uv\cos\phi S-\epsilon uw\sin\phi S = -\epsilon\frac{\partial p}{\partial s}+$$

$$+\left(\frac{2\epsilon}{\mathrm{Rb}}(v\cos\phi - w\sin\phi)+\frac{\epsilon}{\mathrm{Rb}^2}\left((X+1)X_s + ZZ_s\right)\right)h_s +$$

$$+\frac{\eta}{\epsilon \mathrm{Re}_\alpha}\left(\frac{-n\epsilon^3\cos\phi\left(X_sZ_{sss}-Z_sX_{sss}\right)}{h_s^2}\left(\frac{\partial u}{\partial s}+v\cos\phi(X_sZ_{ss}-Z_sX_{ss}\right)-w\sin\phi S\right)+$$

$$+\frac{\epsilon^2}{h_s}\left(-uS^2+\frac{\partial^2 u}{\partial s^2}+2\frac{\partial v}{\partial s}\cos\phi S + v\cos\phi\left(X_sZ_{sss}-Z_sX_{sss}\right)-w\sin\phi\left(X_sZ_{sss}-Z_sX_{sss}\right)-2\frac{\partial w}{\partial s}\sin\phi S\right)+$$

$$+\left(1+2\epsilon n\cos\phi S\right)\frac{1}{n}\frac{\partial u}{\partial n}+h_s\frac{\partial^2 u}{\partial n^2}+\frac{h_s}{n^2}\frac{\partial^2 u}{\partial \phi^2}-\frac{\epsilon}{n}\frac{\partial u}{\partial \phi}\sin\phi S\Bigg)+$$

$$+\frac{1}{\epsilon \mathrm{Re}_\alpha}\left[\frac{2\epsilon^2}{h_s}\frac{\partial \eta}{\partial s}\left(\frac{\partial u}{\partial s}+v\cos\phi\left(X_sZ_{sss}-Z_sX_{sss}\right)-w\sin\phi\left(X_sZ_{sss}-Z_sX_{sss}\right)\right)+\right.$$

$$\left.+\frac{1}{n}\frac{\partial \eta}{\partial \phi}\left(\epsilon u\sin\phi S+\frac{h_s}{n}\frac{h_s}{n}\frac{\partial u}{\partial \phi}+\epsilon\frac{\partial w}{\partial s}\right)+\frac{\partial \eta}{\partial n}\left(\epsilon\frac{\partial v}{\partial s}-\epsilon u\cos\phi S+h_s\frac{\partial u}{\partial n}\right)\right]+$$

$$+\epsilon E_f\left(\beta+1\right)E_s\left[\frac{\partial E_s}{\partial s}+h_s\left(\frac{E_n}{n}+\frac{\partial E_n}{\partial n}\right)+\cos\phi S E_n+\frac{h_s}{n}\frac{\partial E_\phi}{\partial \phi}-E_\phi\sin\phi S\right] \tag{4}$$

$$h_s\left(\epsilon\frac{\partial v}{\partial t}+\epsilon u\cos\phi g+v\frac{\partial v}{\partial n}+\frac{w}{n}\frac{\partial v}{\partial \phi}-\frac{w^2}{n}\right)+\epsilon u\frac{\partial v}{\partial s}-\epsilon u^2\cos\phi S=-\frac{\partial p}{\partial n}h_s-\frac{2\epsilon}{\mathrm{Rb}}h_s u\cos\phi+$$

$$+\left(\frac{\epsilon}{\mathrm{Rb}^2}\cos\phi\left(\left(X+1\right)Z_s-ZX_s+\delta n\cos\phi\right)\right)h_s+\frac{\eta}{\epsilon n\mathrm{Re}_\alpha}\left(\frac{-\epsilon^2 n\cos\phi\left(X_sZ_{sss}-X_{sss}Z_s\right)}{h_s^2}\left(\frac{\partial v}{\partial s}-u\cos\phi S\right)+\right.$$

$$+\frac{\epsilon}{h_s}\left(-v\cos^2\phi S^2+\frac{\partial^2 v}{\partial s^2}-2\frac{\partial u}{\partial s}\cos\phi S-u\cos\phi\left(X_sZ_{sss}-X_{sss}Z_s\right)+w\sin\phi\cos\phi S^2\right)+$$

$$\left.+\left(1+2\epsilon n\cos\phi S\right)\frac{1}{\epsilon n}\frac{\partial v}{\partial n}+\frac{h_s}{n}\frac{\partial^2 v}{\partial n^2}-\frac{1}{n}\left(\frac{\partial v}{\partial \phi}-w\right)\sin\phi S+\frac{h_s}{\epsilon n^2}\left(\frac{\partial^2 v}{\partial \phi^2}-v-2\frac{\partial w}{\partial \phi}\right)\right)$$

$$+\frac{1}{\epsilon \mathrm{Re}_\alpha}\left[\frac{\epsilon}{h_s}\frac{\partial \eta}{\partial s}\left(\epsilon\frac{\partial v}{\partial s}-\epsilon u\cos\phi S+h_s\frac{\partial u}{\partial n}\right)+\frac{\partial \eta}{\partial n}\left(2h_s\frac{\partial v}{\partial n}\right)+\frac{h_s}{n}\frac{\partial \eta}{\partial \phi}\left(\frac{\partial w}{\partial n}-\frac{w}{n}+\frac{1}{n}\frac{\partial v}{\partial \phi}\right)\right]$$

$$+\epsilon E_f\left(\beta+1\right)E_n\left[\frac{\partial E_s}{\partial s}+h_s\left(\frac{E_n}{n}+\frac{\partial E_n}{\partial n}\right)+\cos\phi S E_n+\frac{h_s}{n}\frac{\partial E_\phi}{\partial \phi}-E_\phi\sin\phi S\right] \tag{5}$$

and

$$h_s\left(\epsilon\frac{\partial w}{\partial t}+\epsilon u\sin\phi g+v\frac{\partial w}{\partial n}+\frac{w}{n}\frac{\partial w}{\partial\phi}-\frac{vw}{n}\right)+\epsilon u\frac{\partial w}{\partial s}+$$

$$+\epsilon u^2\sin\phi S=\left(-\frac{1}{n}\frac{\partial p}{\partial\phi}h_s+\frac{2\epsilon}{\mathrm{Rb}}u\sin\phi+\frac{\epsilon}{\mathrm{Rb}^2}\sin\phi\left(ZX_s-(X+1)Z_s-n\cos\phi\right)\right)h_s+$$

$$+\frac{\eta}{\epsilon n\mathrm{Re}_\alpha}\left(\frac{-\epsilon^2 n\cos\phi\left(X_sZ_{sss}-X_{sss}Z_s\right)}{h_s^2}\left(\frac{\partial w}{\partial s}+u\sin\phi S\right)+\right.$$

$$+\frac{\epsilon}{h_s}\left(-w\sin^2\phi S^2+\frac{\partial^2 w}{\partial s^2}+2\frac{\partial u}{\partial s}\sin\phi S+u\sin\phi\left(X_sZ_{sss}-X_{sss}Z_s\right)+v\sin\phi\cos\phi S^2\right)+$$

$$\left.+\left(1+2\epsilon n\cos\phi S\right)\frac{1}{\epsilon n}\frac{\partial w}{\partial n}+\frac{h_s}{\epsilon}\frac{\partial^2 w}{\partial n^2}-\frac{1}{\epsilon}\left(\frac{\partial w}{\partial\phi}+v\right)\sin\phi S+\frac{h_s}{\epsilon n^2}\left(\frac{\partial^2 w}{\partial\phi^2}-w+2\frac{\partial v}{\partial\phi}\right)\right)+$$

$$+\frac{1}{\epsilon\mathrm{Re}_\alpha}\left[\frac{\epsilon}{h_s}\frac{\partial\eta}{\partial s}\left(\epsilon\frac{\partial w}{\partial s}+\epsilon u\sin\phi S+\frac{h_s}{n}\frac{\partial u}{\partial\phi}\right)+\frac{h_s}{\partial n}\frac{\partial\eta}{\partial n}\left(\frac{\partial v}{\partial\phi}-w+n\frac{\partial w}{\partial n}\right)+\frac{2h_s}{n^2}\frac{\partial\eta}{\partial\phi}\left(\frac{\partial w}{\partial\phi}+v\right)\right]+$$

$$\epsilon E_f(\beta+1)E_\phi\left[\frac{\partial E_s}{\partial s}+h_s\left(\frac{E_n}{n}+\frac{\partial E_n}{\partial n}\right)+\cos\phi S E_n+\frac{h_s}{n}\frac{\partial E_\phi}{\partial\phi}-E_\phi\sin\phi S\right] \tag{6}$$

where $S = X_sZ_{ss} - X_{ss}Z_s$, $h_5 = 1 + \epsilon n\cos\phi(X_sZ_{ss} - X_{ss}Zs)$, and $g = Z_{st}X_s - X_{st}Z_s$. The equations for the surface charge, electric field, the first and second tangential stress conditions, the arc-length condition and the kinematic condition are unchanged from those of Alsharif and Parau *et al*. [28]. However, the changes is caused by the power law model of the viscosity term in the overall governing equations. Thus, the normal condition is shown:

$$p-\frac{2\eta}{\mathrm{Re}_\alpha}\frac{1}{\Xi^2}\left(\epsilon^2\left(\frac{\partial R}{\partial s}\right)^2\frac{1}{h_s^3}\left(\frac{\partial u}{\partial s}+\left(v\cos\phi-\sin\phi\right)S\right)+\frac{1}{\epsilon}\frac{\partial v}{\partial n}+\frac{1}{\epsilon R^3}\left(\frac{\partial R}{\partial\phi}\right)^2\left(\frac{\partial w}{\partial\phi}+v\right)-\right.$$

$$-\frac{\epsilon}{h_s}\frac{\partial R}{\partial s}\left(\frac{1}{h_s}\frac{\partial v}{\partial s}+\frac{1}{\epsilon}\frac{\partial u}{\partial n}-\frac{u}{h_s}\cos\phi S\right)+\frac{\epsilon}{Rh_s}\frac{\partial R}{\partial s}\frac{\partial R}{\partial\phi}\left(\frac{1}{\epsilon R}\frac{\partial u}{\partial\phi}+\frac{u}{h_s}\sin\phi S+\frac{1}{h_s}\frac{\partial u}{\partial s}\right)-$$

$$\left.-\frac{1}{\epsilon R}\frac{\partial R}{\partial\phi}\left(R\frac{\partial w}{\partial n}-\frac{w}{R}+\frac{1}{R}\frac{\partial v}{\partial\phi}\right)\right)+\frac{E_f}{2}\left\{Q^2+2(\beta+1)Q\left(\frac{1}{\Xi}\left(-\frac{\partial R}{\partial s}\frac{\epsilon}{h_s}E_s+E_n-\frac{\partial R}{\partial\phi}\frac{1}{R}E_\phi\right)\right)+\right.$$

$$+\beta(\beta+1)\left(\frac{1}{\Xi}\left(-\frac{\partial R}{\partial s}\frac{\epsilon}{h_s}E_s+E_n-\frac{\partial R}{\partial\phi}\frac{1}{R}E_\phi\right)\right)^2+$$

$$\left.+\beta\frac{1}{\left(1+\left(\frac{\partial R}{\partial s}\frac{\epsilon}{h_s}\right)^2\right)}\left(E_s+\frac{\partial R}{\partial s}\frac{\epsilon}{h_s}E_n\right)^2+\beta\frac{1}{\left(1+\left(\frac{\partial R}{\partial\phi}\frac{1}{R}\right)^2\right)}\left(\frac{\partial R}{\partial\phi}\frac{1}{R}E_n+E_\phi\right)^2\right\}=\frac{\kappa}{\mathrm{We}} \tag{7}$$

where

$$\kappa = \frac{1}{h_s}\left(-\epsilon^2 \frac{\partial}{\partial s}\left(\frac{1}{\Xi h_s}\frac{\partial R}{\partial s}\right)+\frac{1}{n}\frac{\partial}{\partial n}\left(\frac{n h_s}{\Xi}\right)-\frac{\partial}{\partial \phi}\left(\frac{h_s}{\Xi n^2}\frac{\partial R}{\partial \phi}\right)\right)$$

and

$$\Xi = \left(1+\frac{\epsilon^2}{h_s^2}\left(\frac{\partial R}{\partial s}\right)^2+\frac{1}{R^2}\left(\frac{\partial R}{\partial \phi}\right)^2\right)^{1/2}$$

Initially, $R(0) = 1$, and $u(0) = 1$ are the conditions leaving us with $R^2u = 1$. The $\hat{\mathrm{Re}}_\alpha = 0(1)$ is regarded thus in Decent *et al*. [37, 42], when $E_0 = Q_0 = 0$. After some calculations, we get the equations at leading order:

$$u_0 u_{0s} = -\frac{1}{\mathrm{We}}\frac{u_{0s}}{2\sqrt{u_0}}+\frac{(X+1)X_s+ZZ_s}{\mathrm{Rb}^2}+\frac{3\hat{\eta}}{\mathrm{Re}_\alpha}\left(\alpha u_{0ss}-\sqrt{u_0}\,u_{0s}^2\right)+$$
$$+E_f\left(2Q_0E_0\sqrt{u_0}+Q_0Q_{0s}+\beta E_0E_{0s}\right) \tag{8}$$

$$(X_sZ_{ss}-X_{ss}Z_s)\left(\frac{(7-\alpha)\hat{\eta}u_{0s}}{2\mathrm{Re}_\alpha}+\frac{\sqrt{u_0}}{\mathrm{We}}-u_0^2\right)+\frac{2}{\mathrm{Rb}}u_0-$$
$$-\frac{(X+1)Z_s-ZX_s}{\mathrm{Rb}^2}-\frac{(\alpha-1)\hat{\eta}}{\mathrm{Re}_\alpha}u_0(X_sZ_{sss}-X_sX_{sss})=0 \tag{9}$$

$$\frac{2Q_0\sqrt{u_0}}{\bar{K}}+\frac{E_0}{u_0}=1 \tag{10}$$

We can write the dimensionless apparent viscosity in the form:

$$\eta = \hat{\eta}+O(\epsilon n)$$

where

$$\hat{\eta} = \left|\sqrt{3}\,u_{0s}\right|^{\alpha-1}$$

The same equations in Alsharif and Parau *et al*. [28] are yielded when $\alpha = 1$. Moreover, when $Q_0 = E_0 = 0$ these equations diminish to similar equations in Parau *et al*. [43]. An extrinsic electric radial field E_∞ can be detected; consequently, we have:

$$E_\infty = E_\infty\frac{(X+1)i+Z\,k}{(X+1)^2+Z^2}$$

where E_∞ is a dimensionless variable, see also Hashemi *et al*. [44] eq. (14). A potential procedure would be to formulate [45]:

$$E_0-\ln\left(\frac{1}{\chi}\right)\left[\frac{\beta}{2}\left(\frac{E_0}{u_0}\right)_{ss}-\sqrt{\beta}\left(\frac{Q_0}{\sqrt{u_0}}\right)_s\right]=E_\infty\frac{(X+1)X_s+ZZ_s}{(X+1)^2+Z^2}$$

where χ being the aspect ratio of the jet, refer to Hohman *et al*. [27], Yarin *et al.* [31] for further information on the case of a uniform electric field, which can be taken here to be $\chi^{-1} = \epsilon$. For simplicity, we took no notice of the second term on the left-hand side of the prior equation:

$$E_0(s) = E_\infty \frac{(1+X)X_s + ZZ_s}{(1+X)^2 + Z^2} \tag{11}$$

$$X_s^2 + Z_s^2 = 1 \tag{12}$$

In this framework, we have four equations in four unknowns which are u_0, X, Z, Q_0, and E_0. To acquire the arrangements of these equations, we utilize the Rounge-Kutta strategy with the goal that we can decide the trajectory of the jet. In figs. 1-3, we plot the trajectory of a rotating liquid jet with the effects of the electric force E_f and the Rossby number, Rb. We can see that these two powers affect the trajectory of power-law fluid jets. The span along the fluid jet has been represented within the sight of different estimations of dimensionless parameter Rossby number and E_∞ , see figs. 4 and 5. In figs. 6 and 7, the surface charge Q_0 and the characteristic field strength E_0 have shown along the liquid jet.

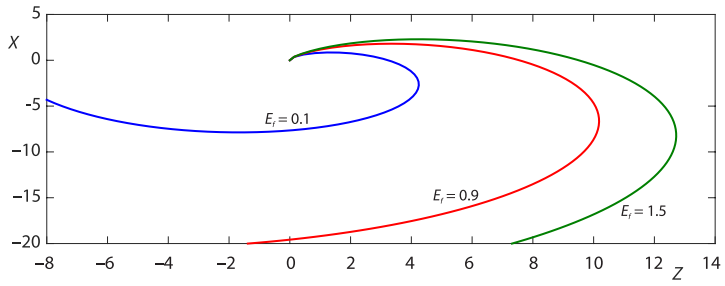

Figure 1. Jet trajectory for three values of Ef, where We = 10, Rb = 1, $\bar{k}$ = 10, E_∞ = 5, and β = 40

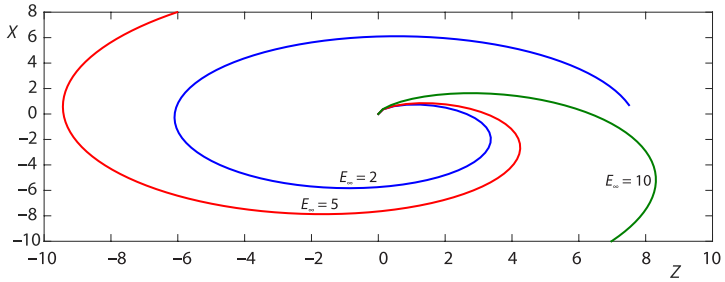

Figure 2. Jet trajectory for different values of E_∞, where Rb = 1, $\bar{k}$ = 10, We = 10 E_f =0.1, and β = 40

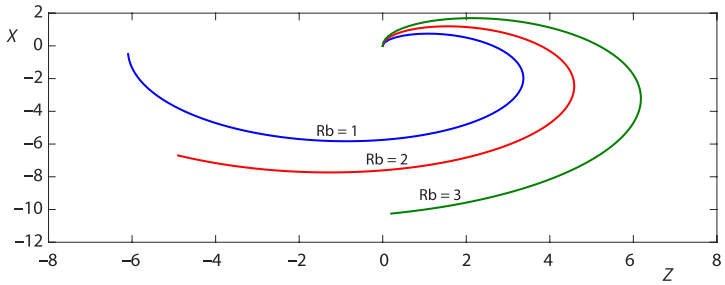

Figure 3. The R_0 against s with three different numbers of Rb, at We = 10, $\bar{k}$ = 10, E_f = 0.1, E_∞ = 2, and β = 40

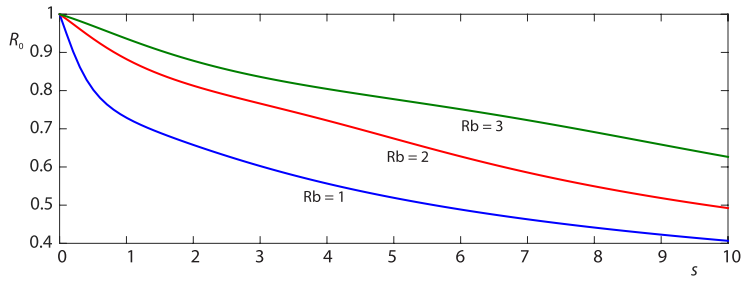

Figure 4. The R_0 against s with three different numbers of Rb, at We = 10, $\bar{k}$ = 10, E_f = 0.1, E_∞ = 2, and β = 40

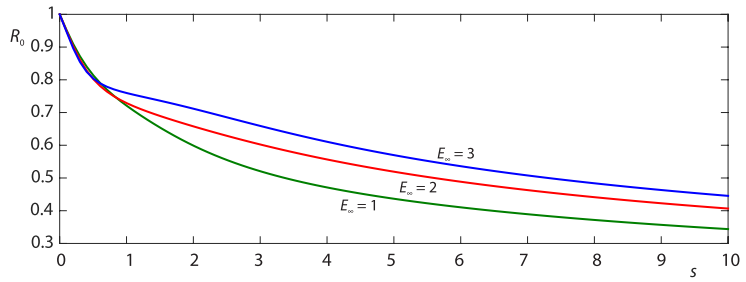

Figure 5. The R_0 against s with three different numbers of E_∞, at We = 10, $\bar{k}$ = 10, E_f = 0.1, Rb = 1, and β = 40

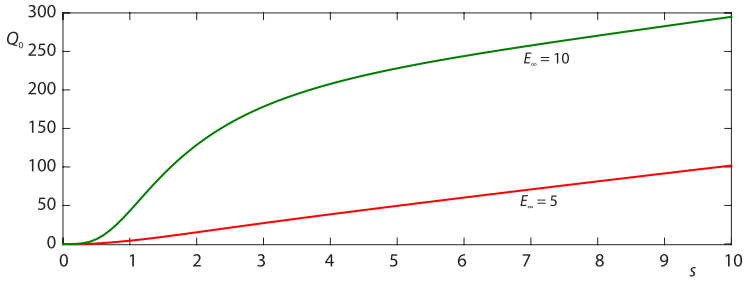

Figure 6. The Q_0 against s with three different numbers of E_∞, at We = 10, $\bar{k}$ = 10, E_f = 0.1, Rb = 1, and β = 40

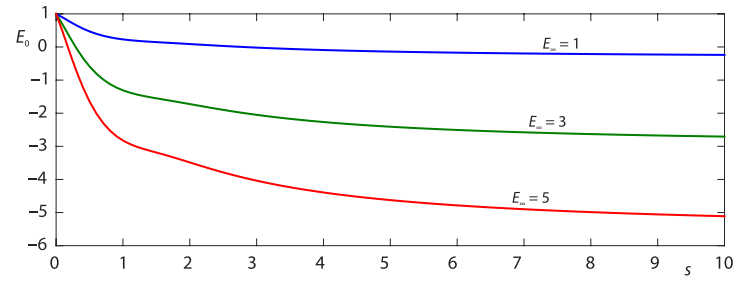

Figure 7. The E_0 against s with three different numbers of E_∞, at We = 10, $\bar{k}$ = 10, E_f = 0.1, Rb = 1, and β = 40

Temporal instability analysis

A small travelling wave mode has been considered around the steady-state answers (7)-(11), that are raveled in the above section, creating a small perturbation in these solutions as shown:

$$(u, R, E, Q) = (u_0, R_0, E_0, Q_0)(s) + \delta(\hat{u}, \hat{R}, \hat{E}, \hat{Q}) exp(i\kappa \bar{s} + \omega \bar{t}) \tag{13}$$

in which $\bar{s}$ = s/ϵ becomes small length scales, $\bar{t}$ = t/ϵ is small time scales, $k = k(s)$, and $w = w(s)$ are the wavenumber and wavelength of the aggravations, and δ is a small constant which is $0 < \delta < \epsilon^2$, see Uddin [46]. The steady-state solutions are indicated by the symbols with subscripts. Supplanting the leading order pressure term $1/R$We with the full curvature expression

$$\left[\frac{1}{R_0 \left(1 + R_{0s}^2\right)^{1/2}} - \frac{\epsilon^2 R_{0ss}}{\left(1 + R_{0s}^2\right)^{3/2}} \right]$$

is needed to exclude the instability of wave modes containing zero wavelength [40]:

$$u_{0t} + u_0 u_{0s} = -\frac{1}{\mathrm{We}} \left[\frac{1}{R_0 (1 + R_{0s}^2)^{1/2}} - \frac{\epsilon^2 R_{0ss}}{(1 + R_{0s}^2)^{3/2}} \right]_s + \frac{(X+1)X_s + ZZ_s}{\mathrm{Rb}^2} +$$
$$+ \frac{3\hat{\eta}}{\mathrm{Re}_\alpha} \left(\alpha u_{0ss} + 2u_{0s} \frac{R_{0s}}{R} \right) + E_f \left(\frac{2}{R} Q_0 E_0 + Q_0 Q_{0s} + \beta E_0 E_{0s} \right) \tag{14}$$

We also have the kinematic condition:

$$R_{0t} + u_0 R_{0s} + \frac{R_0}{2} u_{0s} = 0 \tag{15}$$

and the density equation of surface charge at leading order:

$$\frac{\partial}{\partial t}\left(2R_0 Q_0\right) + \frac{\partial}{\partial s}\left(2R_0 u_0 Q_0 + R_0^2 \bar{K} E_0\right) = 0 \tag{16}$$

The perturbation eq. (12) are used to substitute into the eqs. (10) and (13)-(15). We therefore, get the dispersion relation at leading order which takes the form:

$$\left(\omega + iku_0\right)^3 + \left(\frac{3k^2 f}{\bar{\mathrm{Re}}_\alpha} + \frac{\bar{K}}{\sqrt{\beta}} \right) \left(\omega + iku_0\right)^2 - \left(\frac{k^2 R_0}{2\mathrm{We}} \left(\frac{1}{R_0^2} - k^2 \right) - \frac{3k^2 \bar{K}}{\sqrt{\beta}\,\bar{\mathrm{Re}}_\alpha} - \frac{E_f k^2 Q_0^2}{2} + \right.$$
$$\left. + E_f k^2 \beta E_0^2 \right) \left(\omega + iku_0\right) - \left(\frac{k^2 R_0 \bar{K}}{2\mathrm{We}\sqrt{\beta}} \left(\frac{1}{R_0^2} - k^2 \right) + \frac{R_0 E_f k^2 \bar{K} Q_0^2}{2\sqrt{\beta}} + E_f k^2 \bar{K} \sqrt{\beta} E_0^2 \right) = 0 \tag{17}$$

where

$$f = \alpha \left| \sqrt{3} u_{0s} \right|^{\alpha - 1}$$

One may find that once there is no electric field influenced, meaning that $\bar{k} = Q_0 = E_0 = 0$, the eigenvalue relation (16):

$$\left(\omega + iku_0\right)^2 + \frac{3k^2}{\bar{\mathrm{Re}}} \left(\omega + iku_0\right) - \left[\frac{k^2 R_0}{2\mathrm{We}} \left(\frac{1}{R_0^2} - k^2 \right) \right] = 0 \tag{18}$$

which gives the eigenvalue relationship of viscous liquid fluids that have been identified by Decent *et al.* [41]. A plot has been shown in fig. 8 to present the connection between the development rate ω, and the wavenumber k for contrasting estimations of the electric power parameter E_f, and it was noticed that once we increment this non-dimensionless parameter, the development slope increments. In figs. 9 and 10, we plot the connection between the development rate ω and the electric field parameter E_f for shear-thinning ($\alpha = 0.5$), and shear thickening fluid jets ($\alpha = 1.3$) at different estimations of the Rossby number, individually. From these two figures, we can analyse that a diminishing in the Rossby number (which means expanding the rotation rate) prompts an expansion in the development rate. We likewise made an examination between shear thinning and shear thickening fluid curved jets within the sight of an electric field at Rb = 1 and 1.5, see fig. 11 . We hence found that shear-thinning fluid jets have more development rate than shear thickening fluid jets at a fixed Rossby number.

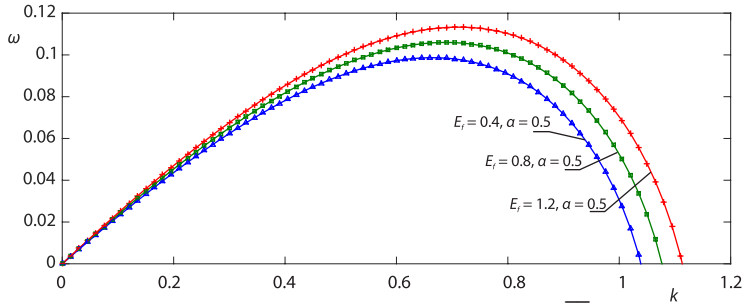

Figure 8. The *k vs.* ω for different values of *Ef*, where $\overline{\mathrm{Re}} = 30$, We = 10, $\bar{k} = 5$, and $\beta = 0.01$

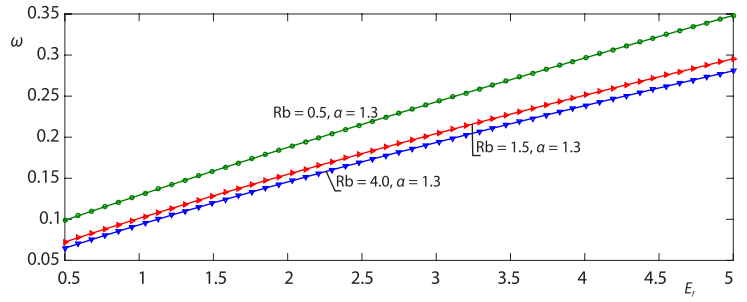

Figure 9. The ω *vs.* E_f for different values of β, where $\overline{\mathrm{Re}} = 3$, We = 10, $\bar{k} = 0.5$, and $\beta = 0.1$, and $E_f = 0.2$ at $s = 1$

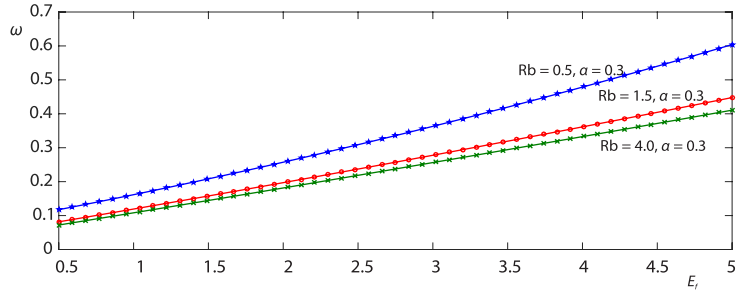

Figure 10. The ω *vs.* E_f for different values of β, where $\overline{\mathrm{Re}} = 3$, We = 10, $\beta = 0.1$, $\bar{k} = 0.5$, and $E_f = 0.2$ at $s = 1$

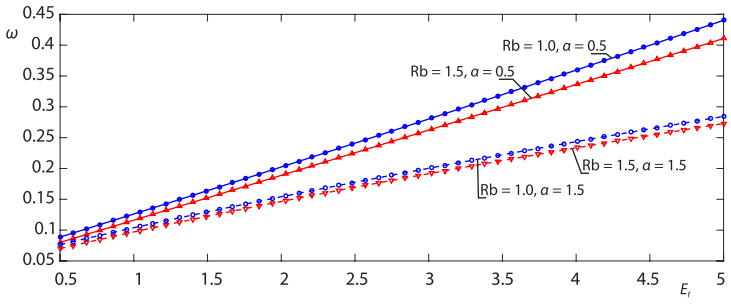

Figure 11. The ω *vs.* E_f for different values of β, where $\overline{\mathrm{Re}} = 3$, We = 10, $\beta = 0.1$, $\bar{k} = 0.5$, and $E_f = 0.2$ at $s = 1$

Conclusions

In this paper, a power law non-Newtonian leaky dielectric curved jet's behaviour in an external electric field was examined to determine how temporal linear instability may be predicted. The continuity, momentum, and electric potential equations are all parts of the electro-hydrodynamic equations.

Alsharif and Parau *et al*. [28] investigated the centrifugal spinning viscus jet in the presence of electric field, and they have found that the trajectory of a rotating liquid jet with the influence of the electric force E_f and the Rossby number. They also have found out that these two powers affect the trajectory of viscous fluid jets. In addition, the span along the fluid jet has been represented within the sight of different estimations of dimensionless parameter Rossby number and E_∞. Here, power law model plays an important role for the trajectory and temporal instability of curved viscous liquid jets in the presence of an external electric field.

From this linear instability, we have derived the dispersion relation examine growth rates connected with a shear thinning and a shear thickening of fluids. From this derived dispersion relation, we can see that we have numerous parameters, can have an impact on the mechanisms underlying the linear instability of these viscous curved fibers with the electric field. As a result, we have discovered that the electric force parameter and rotation rate can alter the rates at which disturbances for shear thinning and shear thickening liquids grow. We have also discovered that the rotation rate and the electric field parameter can change the growth rates of aggravations for shear thinning and shear thickening fluids. The span along the fluid jet has been represented within the sight of different estimations of dimensionless parameters Rossby number and E_∞, see figs. 4 and 5. The surface charge Q_0 and the characteristic field strength E_0 have also shown along the liquid jet. Therefore, we have observed that these non-dimensional parameters affect the trajectory of this problem. we show the connection between the development rate ω and the electric field parameter E_f for shear-thinning ($\alpha = 0.5$), and shear thickening fluid jets ($\alpha = 1.3$) at different estimations of the Rossby number, individually. It is clear from these two figures that a diminishing in the Rossby number (which means expanding the rotation rate) prompts an expansion in the development rate.

Acknowledgment

Alsharif would like to thank the researchers at Taif University, who supported project number (TURSP-2020/96) at Taif University, Taif, Saudi Arabia.

References

[1] Savart, F., a Mémoire sur la constitution des veines liquides lancees par des orifices circulaires en mince paroi, *Ann. de Chim., 53* (1833), pp. 337-386
[2] Plateau, J., *Statique Experimentale et theortique des liquides soumis aux seules forces moleculaires*, Gauthier Villars, Paris, France, II, 319, 1873
[3] Rayleigh, W. S., On the Instability of Jets, *Proc. Lond. Math. Soc.*, *10* (1878), 4
[4] Middleman, S., Stability of a Viscoelastic Jet, *Chem. Eng. Sci*., *20* (1965), 12, pp. 1037-1040
[5] Renardy, M., A Numerical Study of the Asymptotic Evolution and Breakup of Newtonian and Viscoelastic Jets, *Journal Non-Newtonian Fluid Mech*., *59* (1995), 2-3, pp. 267-282
[6] Goldin, M., *et al.*, Breakup of a Viscoelastic Fluid, *Journal Fluid Mech*., *38* (1969), pp. 689-711
[7] Brenn, G., *et al.*, Linear Analysis of the Temporal Instability of Axisymmetrical Non-Newtonian Liquid jets, *International Journal of Multi-phase Flow*, 26 (2000), 10, pp. 1621-1644
[8] Larson, R. G., *Constitutive Equation for Polymer Melts and Solutions*, in: Butterworths Series in Chemical Eng., Elsavier, Amsterdam, The Netherlands, 1988
[9] Schummer, P., Thelen, H. G., Break-up of a Viscoelastic Liquid Jets, *Rheol. Acta*, *27* (1988), Jan., pp. 39-43
[10] Larson, R. G., Instabilities in Viscoelastic Flows, *Rheol*. *Act*a, *31* (1992), May, pp. 213-263
[11] Fontelos, M. A., Break-up and no Break-up in a Family for the Evolution of Viscoelastic Jets, *Z. Angew. Math. Phy*s., *54* (2003), Jan., pp. 84-111
[12] Davidson, M. R., *et al.*, Simulation of Pendant Drop Formation of a Viscoelastic Liquid, *Korea-Australia Rheology Journal*, *18* (2006), 2, pp. 41-49
[13] Fontelos, M. A., Li, J., On the Evolution and Rupture of Filaments in Giesekus and FENE Models, *Journal Non-Newtonian Fluid Mech*., *118* (2004), 1, pp. 1-16
[14] Liu, Z., Liu, Z., Instability of a viscoelastic liquid jet with axisymmetric and asymmetric disturbance, *International Journal of Multi-phase Flow*, *34* (2008), 1, pp. 42-60
[15] Ardekani, A. M., *et al*., Dynamics of Bead Formation, Filament Thinning and Breakup in Weakly Viscoelastic Jets, *Journal Fluid Mech*., *665* (2010), Dec., pp. 46-56
[16] Cheong, B. S., Howes, T., Capillary Jet Instability under Influence of Gravity, *Chemmical Engineering Science*, *59* (2004), 11, pp. 2145-2157
[17] Morrison, N. F., Harlen, O. G., Viscoelasticity in inkjet printing, *Rheol*. *Acta*, *49* (2010), Jan., pp. 619-632
[18] Sauter, U., S., Buggisch, H., W., Stability of Initially Slow Viscous Jets Driven by Gravity, *Journal Fluid Mech*., *533* (2005), June, pp. 237-257
[19] Divvela, M. J., *et al.,* Discretized Modelling for Centrifugal Spinning of Viscoelastic Liquids, *Journal of Non-Newtonian Fluid Mechanics*, *247* (2017), Sept., pp. 62-77
[20] Alsharif, A. M., Instability of non-Newtonian Liquid Jets in Centrifugal Spinning with Surfactants, *Fluid Dynamics Research*, *51* (2019), 3, 035510
[21] Taghavi, S. M., Larson, R. G., Regularized Fhin-Fiber Model for Nanofiber Formation by Centrifugal Spinning, *Physical Review E*, *89* (2014), 2, 023011
[22] Alsharif, A. M., *et al*., Instability of Viscoelastic Curved Jets, *Appl. Math. Modell*., *39* (2015), 14, pp. 3924-3938
[23] Riahi, D. N., Modelling and computation of non-linear rotating polymeric jets during force spinning process, *International Journal of Non-linear Mechanics*, *92* (2017), June, pp. 1-7
[24] Noroozi, S., *et al*., Regularized String Model for Nanofibre Formation in Centrifugal Spinning Methods, *Journal, Fluid. Mech*., *822* (2017), July, pp. 202-234
[25] Rogalski, J. J., *et a*l., Rotary Jet Spinning Review a Potential High Yield Future for Polymer Nanofibers, *Nanocomposites*, *3* (2017), 4, pp. 97-121
[26] Hohman, M. M., *et al*., Electrospinning and Electrically Forced Jets, I. *Stability Theory: Phys. Fluids*, *13* (2001), 8, 2201
[27] Hohman, M. M, *et al*., Electrospinning and Electrically Forced Jets: II. *Applications Phys. Fluids*, *13* (2001), 8, 2221
[28] Alsharif, A. M., Parau, E. I., Temporal Instability of Curved Viscous Fibers with a Radial Electric Field, *IMA Journal of Applied Mathematics*, *87* (2022), 3, pp. 380-406
[29] Feng, J. J., Stretching of a Straight Electrically Charged Viscoelastic Jet, *J. Non-Newtonian Fluid Mech.*, *116* (2003), 1, pp. 55-70
[30] Reneker, D. H., *et al*., Bending Instability of Electrically Charged Liquid Jets of Polymer Solutions in Electrospinning, *Journal Appl. Phys*., *87* (2000), 9, pp. 4531-4547
[31] Yarin, A. L., *et al.,* 2001, Bending Instability in Electrospinning of Nanofibers, *Journal Appl. Phys*., *89* (2001), 5, pp. 3018-3026

[32] Carroll, C. P., Joo, Y. L., Axisymmetric Instabilities of Electrically Driven Viscoelastic Jets, *Journal Non-Newtonian Fluid Mech.*, *153* (2006,), 2-3, pp. 130-148
[33] Chang, W. M., *et al*., The Combination of Electrospin-Ning and Forcespinning: Effects on a Viscoelastic Jet and a Single Nanofiber, *Chemical Engineering Journal*, *244* (2014), May, pp. 540-551
[34] Liao, C. C., *et al*., Stretching-Induced Crystallinity and Orientation of Polylactic Acid Nanofibers with Improved Mechanical Properties Using an Electrically Charged Rotating Viscoelastic Jet, *Polymer*, *52* (2011), 19, pp. 4303-4318
[35] Riahi, D. A., On Non-Linear Rotating Electrified Non-Newtonian Jets, *International Journal of Non-Linear Mechanic*s, *109* (2019), Mar., pp. 166-171
[36] Wallwork, I. M., The Trajectory and Stability of a Spiralling Liquid Jet, Ph. D. thesis, University of Birmingham, Birmingham, UK, 2022
[37] Decent, S. P., *et al*., Free Jets Spun from a Prilling Tower, *Journal of Engineering Mathematics*, *42* (2002), Apr., pp. 265-282
[38] Melcher, J. R., Taylor, G. I., Electrohydrodynamics: A Review of the Role of Interfacial Shear Stresses, *Annual Review of Fluid Mechanics*, *1* (1969), Jan., pp. 111-146
[39] Saville, D. A., Electrohydrodynamics: The Taylor-Melcher Leaky Dielectric Model, *Annual Review of Fluid Mechanics*, *2*9 (1997), Jan., pp. 27-64
[40] Eggers, J., Non-Linear Dynamics and Breakup of Free Surface Flows, *Rev. Mod. Physis*, *69* (1997), 3, pp. 865-929
[41] Decent, S. P., *et al*., The Trajectory and Stability of a Spiralling Liquid Jet – Part II: Viscous Theory, *Appl. Math. Modelling*, *33* (2007), 12, pp. 4283-4302
[42] Uddin, J., *et al*., The Instability of Shear Thinning and Shear Thickening Spiralling Liquid Jets: Linear Theory, *ASME J. of Fluids Eng*., *128* (2006), 5, pp. 968-975
[43] Parau, E. I., *et al.*, Non-Linear Viscous Liquid Jets from a Rotating Orifice, *Journal of Eng. Maths*., *57* (2007), Dec., pp. 159-179
[44] Hashemi, A. R., *et al*., Numerical and Experimental Study on the Steady Cone-Jet Mode of Electro-Centrifugal Spinning, *Phys. Fluids*, *30* (2018), 017103
[45] Stone, H. A., *et al*., Drops with Conical ends in Electric and Magnetic Fields, *Proc. R. Soc. Lond. A*, *455* (1999), 1991, pp. 329-347
[46] Uddin, J., An Investigation into Methods to Control Breakup and Droplet Formation in Single and Compound Liquid Jets, Ph. D. thesis, University of Birmingham, Birmingham, UK, 2007

Paper submitted: August 15, 2022
Paper revised: October 20, 2022
Paper accepted: October 30, 2022